Smart Materials and Structures

PAPER • **OPEN ACCESS**

Singular spectrum analysis and fuzzy entropy-based damage detection on a thin aluminium plate by using PZTs

To cite this article: Huijun Song *et al* 2022 *Smart Mater. Struct.* **31** 035015

OPEN ACCESS
IOP Publishing
Smart Materials and Structures
Smart Mater. Struct. **31** (2022) 035015 (14pp)
https://doi.org/10.1088/1361-665X/ac4e53

Singular spectrum analysis and fuzzy entropy-based damage detection on a thin aluminium plate by using PZTs

Huijun Song[1], Ming Xiang[2], Guangtao Lu[1,*] and Tao Wang[3]

[1] Key Laboratory for Metallurgical Equipment and Control of Ministry of Education, Wuhan University of Science and Technology, Wuhan 430081, People's Republic of China
[2] Hubei Key Laboratory of Mechanical Transmission and Manufacturing Engineering, Wuhan University of Science and Technology, Wuhan 430081, People's Republic of China
[3] Precision Manufacturing Institute, Wuhan University of Science and Technology, Wuhan 430081, People's Republic of China

E-mail: luguangtao@wust.edu.cn

Received 18 September 2021, revised 13 January 2022
Accepted for publication 24 January 2022
Published 4 February 2022

Abstract

In this research, a new method based on singular spectrum analysis (SSA) and fuzzy entropy is developed for damage detection on thin wall-like structures, and the normalized fuzzy entropy is employed as an indicator to identify the severity of the damage. The lead zirconate titanate (PZT) transducers are used in this research to generate and detect the Lamb waves. During the detection, the collected signals from the PZT sensors are firstly decomposed and reconstructed by SSA to extract the feature of the damage, and then the reconstructed signals with the feature of the damage are processed to obtain the normalized fuzzy entropy. An experimental setup of an aluminium plate with added magnets is fabricated to validate the proposed method. The experimental results show that when magnets are attached on the aluminium plate, the normalized fuzzy entropy is smaller than that when there are no magnets. That is because when magnets are placed on the plate, the movement and some vibration modes of Lamb waves are disturbed by the added magnets and this disturbing effect can be enhanced by increasing the number and locations of the added magnets, and eventually the complexity and nonlinearity of the waves are weakened. The experimental results of a single damage with different number of magnets indicate that the normalized fuzzy entropy decreases linearly as the number of the added magnets increases, which demonstrates that the proposed method can be used to detect the severity of the damage. Moreover, the experimental results of multi-damage on different locations indicate that the normalized fuzzy entropy is relevant with both the total number and locations of the added magnets. The normalized fuzzy entropy decreases linearly as the total number of the magnets increases, and the entropy of a single damage is smaller than that of the multi-damage with the same total number of magnets, which demonstrates that the proposed method also can be used for multi-damage detection on a thin plate. This study provides us a new approach to identifying a single or multiple damages on thin wall-like structures.

* Author to whom any correspondence should be addressed.

Keywords: Lamb waves, lead zirconate titanate (PZT), singular spectrum analysis (SSA), fuzzy entropy

(Some figures may appear in colour only in the online journal)

1. Introduction

Thanks to their good mechanical properties, light weight, and low cost, thin wall-like structures have been increasingly used [1], such as high-pressure gas cylinders, oil pipelines, and aerospace structures. During their service life, the thin wall-like structures will inevitably suffer various types of structural damages, such as delamination [2–4], holes [5–7], cracks [8, 9] and so on, under the effect of the alternating load [10], chemical corrosion [11, 12], and environmental factors [13]. Eventually, these damages will threaten their performance and safety [14] if they are not identified in early age. Therefore, structural health monitoring (SHM) for early damages or damages with a small size on thin wall-like structures is essential.

Nowadays, due to their ability of relative long-distance propagation and small-scale defect identification, Lamb waves have demonstrated great potential and received much attention in SHM of thin wall-like structures [15]. However, due to the strong dispersive characteristics of Lamb waves, the waves usually display strong nonlinearity and disorder themselves as they travel in a structure [16]. Moreover, the existence of structural damages, including cracks, delamination and imperfect contacts, usually has an influence on the local stiffness of the structure, and eventually it may bring about disorder or nonlinearity to the waves and change the complexity of the received signals [17–20]. Therefore, to detect the structural damages effectively and accurately, two crucial problems which need to be overcome are how to separate and enhance the nonlinear and disorder information of the damage from the received signals, and how to develop an indicator or feature with high sensitivity and resolution to quantify the nonlinearity and disorder related to the structural damage.

In the last decades, with the help of the rapid development and successful applications of time series analysis methods, many signal processing technologies, including filtering [21], correlation analysis [22], fast Fourier transform [23, 24], short-time Fourier transform [25, 26], empirical mode decomposition (EMD) [27, 28], ensemble EMD [29], variational mode decomposition (VMD) [30] and other methods [31–36], are implemented to enhance or extract the feature of the damage from the complex signals in Lamb wave-based SHMs. Moreover, some researches recently indicate that the singularities of the signal are related to some features of the structural damage, and these singularities are usually obtained by singular spectrum analysis (SSA). Therefore, SSA shows distinguishable applications in different structures including concrete structures [37] and thin plates [38] for feature extraction. Oliveira *et al* [39] decomposed the signal firstly by SSA and then reconstructed the signal. After this processing, the root mean square deviation (RMSD) and correlation coefficient deviation metric (CCDM) features of the simulated mass damage on a thin plate were enhanced. Similarly, Liu and Yan [38] located the hole damage in an aluminium plate by reconstructed signals with different components which were decomposed by SSA. Overall, the excellent performance of SSA at feature extracting may provide us a new approach to separate the useful information related the structural damage from the complex signals.

Meanwhile, entropy, including Shannon entropy [40], Wiener entropy [41, 42], approximate entropy [43], sample entropy [44], fusion entropy [45], wavelet entropy [20, 46, 47] and multi-scale cross entropy [48–50], is effective as a quantitative measure of the uncertainty or disorder of a signal, and the entropy is usually employed as a feature to describe the nonlinearity of different types of signals. Notably, entropy is already being introduced to analyse the ultrasonic signals, and it is used as a new feature to take the place of the conventional statistical indices, such as the RMSD, the CCDM [39], Pearson correlation coefficient [51] and the *n*th normalized correlation moment [23], for damage estimation. Burud and Kishen [47] succeeded detecting the damage of concrete under flexure with the help of wavelet entropy. Castro *et al* [52] took the spectrum entropy as a damage index to identify the simulated mass on a composite fibre reinforced polymers plate.

In this paper, to solve the two problems as mentioned above, a new damage detection method by combining SSA and fuzzy entropy (fuzzyEn) is proposed to detect different damages on an aluminium plate. Firstly, SSA is used to extract the nonlinear information related to the damages, then some components of the extracted signal are selected to reconstruct and calculate the fuzzy entropy, and at last the fuzzy entropy is employed as a new indicator to characterize the severity of the damage.

The rest of this paper is organized in the following manner. Section 2 introduces the theoretical background of SSA and fuzzy entropy and presents the procedure of the proposed method. Section 3 describes the experimental setup and procedures to validate the proposed method. Section 4 analyses the experimental results in detailed. At last, section 5 concludes the paper with recommendation for future work.

2. Theoretical fundamentals

The overall procedure of the SSA and fuzzy entropy-based method is described in figure 1. After the original signal is obtained by the active sensing method, it is decomposed by SSA to extract the features related to the structural damage, and some components are selected to reconstruct a new signal which contains the nonlinear information of the damage. Subsequently, the fuzzy entropy is calculated by the reconstructed signal and it is chosen as an indicator to evaluate the severity of the damage.

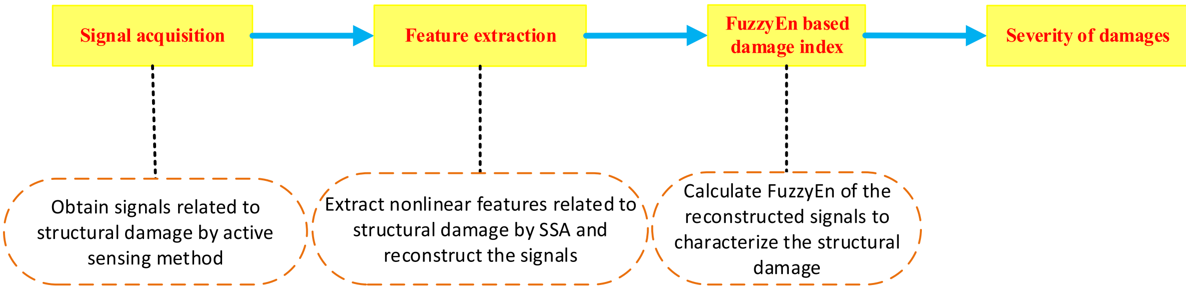

Figure 1. Flowchart of the SSA and fuzzy entropy-based damage detection method.

2.1. SSA

As a nonparametric estimation method, SSA possesses the strong capacity of analysing nonlinear signals with narrow-banded components [53–55]. Therefore, SSA is employed in this paper to analyse the Lamb wave signals which have strong nonlinearity due to frequency dispersion. The procedure of SSA is described in detailed in the following.

2.1.1. Step 1: Embedding. Given a one-dimensional discrete-time series $x(n)$ with length N, and it is embedded into $K = N - M + 1$ vectors $\mathbf{x}(i) = (x(i),\ldots,x(i+M-1))^{\mathrm{T}}$ $(i = 1,\ldots,N-M+1)$ by an embedding dimension $M(M < N/2)$. The lagged K vectors are merged into the trajectory matrix $\mathbf{X}$ of the series $x(n)$, and the matrix is given as

$$\mathbf{X} = [\mathbf{x}(1)\,\mathbf{x}(2)\cdots\mathbf{x}(N-M+1)] = \begin{bmatrix} x_1 & x_2 & \cdots & x_{N-M+1} \\ x_2 & x_3 & \cdots & x_{N-M+2} \\ \vdots & \vdots & & \vdots \\ x_M & x_{M+1} & \cdots & x_N \end{bmatrix}. \quad (1)$$

2.1.2. Step 2: Singular value decomposition. Applying the singular value decomposition of the covariance matrix $\mathbf{X}^{\mathrm{T}}\mathbf{X}$ of the trajectory matrix results in:

$$\mathbf{X}^{\mathrm{T}}\mathbf{X} = \mathbf{V}\sum\mathbf{V}^{\mathrm{T}} \quad (2)$$

where $\sum = \mathrm{diag}\{\lambda_1,\ldots,\lambda_i\ldots,\lambda_K\}$ is the diagonal matrix of the eigenvalues, which are sorted in descending order; and $\mathbf{V} = (V_1, V_2,\ldots,V_M)$ is the corresponding orthogonal matrix of the eigenvectors.

Therefore, the trajectory matrix can be theoretically expressed by the eigenvectors as

$$\mathbf{X} = \mathbf{X}_1 + \mathbf{X}_2 + \cdots + \mathbf{X}_d \quad (3)$$

where $\mathbf{X}_i = \sqrt{\lambda_i}V_iU_i'$ $(i = 1,2,\ldots,d)$ is called the elementary matrix of the trajectory matrix, $U_i = \mathbf{X}'V_i/\sqrt{\lambda_i}$ and d is the rank of the trajectory matrix $\mathbf{X}$.

The ratio $\alpha_i = \lambda_i/\sum_{i=1}^{d}\lambda_i$ is the contribution of the elementary matrix $\mathbf{X}_i$ to the trajectory matrix $\mathbf{X}$, and a larger value of the coefficient α_i means that the corresponding matrix $\mathbf{X}_i$ contains more features or information of the original signal.

2.1.3. Step 3: Reconstruction of the signal related to the structural damage. To extract the components related to the structural damage, the first m $(m < d)$ elementary matrices $\mathbf{X}_i$ are selected based on the coefficient α_i to assemble a new matrix $\mathbf{Y}$

$$\mathbf{Y} = \mathbf{X}_1 + \mathbf{X}_2 + \cdots + \mathbf{X}_m. \quad (4)$$

At last, the signal $y(n)$ can be reconstructed by the matrix $\mathbf{Y}$ using the method of diagonal averaging [56].

2.2. Fuzzy entropy

Since the inception of fuzzy entropy (fuzzyEn) by Chen *et al* [57], it has been widely used in nonlinear and nonstationary signal analysis due to its good statistical stability and ability of measuring the complexity and nonlinearity of the signal. In this study, fuzzy entropy is used as an indicator to measure the nonlinearity related to the structural damage.

After the original signal is extracted and reconstructed by SSA, the reconstructed signal is further processed to obtain the fuzzy entropy by six steps as below.

Step 1: Construct p-dimensional vectors $\mathbf{Y}_i^p$ from the processed signal $y(n)$ by an initialization mode dimension p, and the vector is given by

$$\mathbf{Y}_i^p = \{y(i), y(i+1),\ldots,y(i+p-1)\} - y_0(i)$$
$$i = 1,\ 2\cdots N-p+1 \quad (5)$$

where p is the mode dimension, and the optimal value of p is usually obtained by the trial calculation, and $y_0(i)$ is defined by

$$y_0(i) = \frac{1}{p}\sum_{j=0}^{p-1} y(i+j). \quad (6)$$

Step 2: Define the distance d_{ij}^p between two vectors $\mathbf{Y}_i^p$ and $\mathbf{Y}_j^p$ as the maximum absolute difference of the two corresponding elements, and the distance is given by

$$d_{ij}^p = d\left[\mathbf{Y}_i^p, \mathbf{Y}_j^p\right] = \max_{k\in(0,m-1)} |[y(i+k) - y_0(i)] - [y(j+k) - y_0(j)]|$$
$$i,j = 1,2\cdots N-p \,\mathrm{and}\, i \neq j. \quad (7)$$

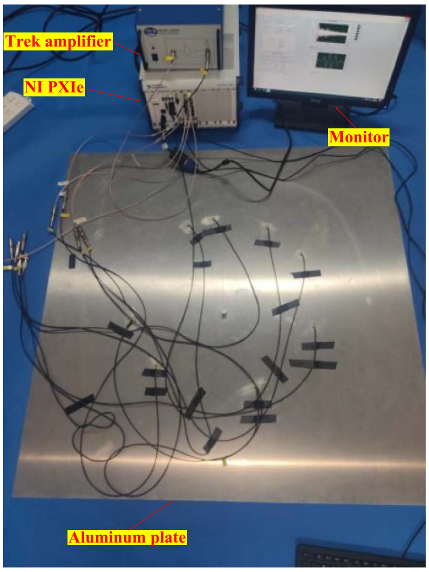

(a) The whole experimental setup

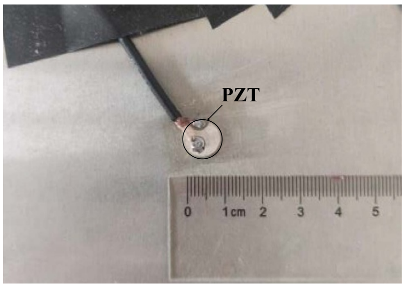

(b) The enlarged view of the PZT

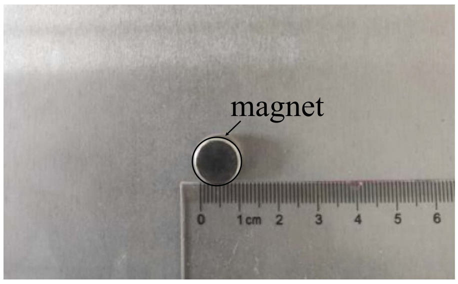

(c) The enlarged view of the simulated damage

Figure 2. Experimental setup.

Step 3: Compute the similarity between the two vectors $\mathbf{Y}_i^p$ and $\mathbf{Y}_j^p$ by using a fuzzy membership function and the similarity is expressed as

$$d_{ij}^p = \mu(d_{ij}^p, q, r) = \mathrm{e}^{-\left(d_{ij}^p/r\right)^q} \tag{8}$$

where $\mu(d_{ij}^p, q, r)$ is the fuzzy membership function and it is usually selected as an exponential function, and q and r are the boundary gradient and threshold of the fuzzy member function, respectively. In this paper, q is chosen as 2, and r is set to be 0.15 of the standard deviation of the original signal [58].

Step 4: Calculate $\phi^p(q,r)$ as

$$\phi^p(q,r) = \frac{1}{N-p}\sum_{i=1}^{N-p}\left(\frac{1}{N-p-1}\sum_{\substack{j=1\\ j\neq i}}^{N-p} d_{ij}^p\right). \tag{9}$$

Step 5: Calculating $\phi^{p+1}(q,r)$ by repeating steps (1)–(4) gives

$$\phi^{p+1}(q,r) = \frac{1}{N-p}\sum_{i=1}^{N-p}\left(\frac{1}{N-p-1}\sum_{\substack{j=1\\ j\neq i}}^{N-p} d_{ij}^{p+1}\right). \tag{10}$$

Step 6: The fuzzy entropy is obtained as

$$\mathrm{FuzzyEn}(p, q, r, N) = \ln\phi^p(q,r) - \ln\phi^{p+1}(q,r). \tag{11}$$

To reduce the adverse influence of the lead zirconate titanate (PZT)'s location on the fuzzy entropy, the fuzzy entropy in equation (12) is normalized by the fuzzy entropy when there is no damage, and the normalized fuzzy entropy is expressed as

$$\mathrm{FuzzyEn}_{\mathrm{norm}}(p, q, r, N) = \frac{\mathrm{FuzzyEn}\,(p, q, r, N)}{\mathrm{FuzzyEn}_{\mathrm{nodamage}}(p, q, r, N)} \tag{12}$$

where $\mathrm{FuzzyEn}_{\mathrm{nodamage}}(p, q, r, N)$ is the fuzzy entropy of the structure without a damage.

In this research, and the normalized fuzzy entropy is used as an indicator to identify the structural damage.

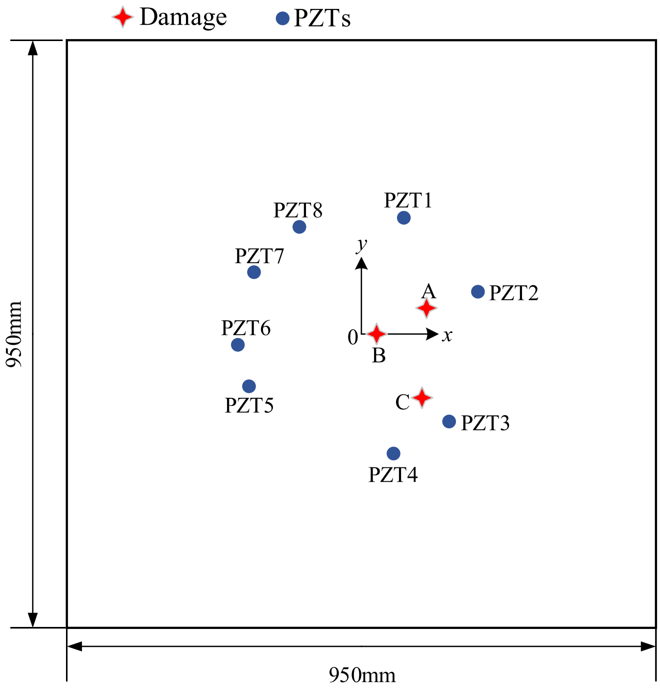

Figure 3. Locations of the PZTs and simulated damage on the aluminium plate.

Table 1. Locations of eight PZT discs.

PZT	Coordinate (mm, mm)
PZT1	(137, 376)
PZT2	(376, 137)
PZT3	(283, −283)
PZT4	(104, −386)
PZT5	(−363, −169)
PZT6	(−399, −35)
PZT7	(−346, 200)
PZT8	(−200, 346)

3. Experimental setup

To verify the method proposed in this research, an experimental setup is designed. As shown in figure 2(a), the experimental setup is mainly composed of an aluminium plate (Aluminium 6061), a data acquisition system (Ni PXIe 8840 chassis with an Ni PXIe-5423 40 MHz bandwidth arbitrary waveform generator and an Ni PXIe-5172 eight-channel oscilloscope), a high-frequency piezoelectric amplifier with 0–2.6 MHz bandwidth and a fixed 50 gain (Trek Model 2100H) and a monitor.

As shown in figure 3, the size of the aluminium plate is 950 mm $\times$ 950 mm $\times$ 1.5 mm. To excite and receive the ultrasonic signals, eight PZT discs (shown in figure 2(b)) with a size of Φ12 mm $\times$ 1 mm are bonded on the plate by epoxy resin, and the locations of the discs are listed in table 1. PZT type of transducers are used in this research due to their advantages of high piezoelectric effects [59], wide bandwidth [60] and ease of installation [61–63].

To reduce the number of the modes of Lamb waves which are excited in the plate, a 280 kHz five-cycle sinusoidal pulse tuned by a Hanning window is selected based on the theory of tuned Lamb waves [64, 65]. Moreover, to collect more nonlinear information of the reflection waves, including the ones that only reflect at the damage and the ones that scatter successively at the boundaries of the damage and the aluminium plate, the recording time should be relative long, and it is set to be 0.0025 s. The excitation pulse in time and frequency domains is plotted in figure 4.

During the experiment, the tuned pulse is firstly generated by the NI PXIe-5423 generator, then amplified by the Trek piezoelectric amplifier and at last sent to one of the eight PZT actuators to excite Lamb waves. The Lamb waves are detected by the left seven PZT sensors and collected by the NI PXIe-5172 oscilloscope.

In the experiments, as shown in figures 2 and 3, to simulate different structural damage, different number of magnets are attached to the aluminium plate on three locations. The three locations of the simulated damages are listed in table 2. As shown in table 3, 18 different types of damage, including single damage (A1–A4, B1–B4 and C1–C4) and multi-damage (M1–M3), are tested and detected by the proposed methods. In the third column of table 3, 'A', 'B' and 'C' are the locations where the magnets are attached, and the number of the magnets at the corresponding location is listed in the fourth column. For example, multi-damage M3 means two magnets and one magnet are attached on location 'A' and 'B', respectively.

In addition, to reduce the adverse effect of electromagnetic interference and temperature on the experimental data, the whole test is conducted in laboratory with the same ambient temperature.

4. Experimental results on the aluminium plate

4.1. Selection of the coefficients

After the ultrasonic signals are obtained, they are processed as described in section 2. In this paper, the embedding dimension M in SSA is chosen as 80. During the processing, to obtain the optimal values of m in SSA, the summation of the coefficient α_i of the first i eigenvalues is plotted in figure 5. Figure 5 shows that the summation of the first eight eigenvalues is larger than 99%, which demonstrates that first eight eigenvalues contain the main features of the signal. Therefore, the value of m is selected as 8 to reconstruct the signal in this study [66].

Moreover, figure 6 plots the curves of the fuzzy entropy of different damages versus the mode dimension p in equation (12). Figure 6 indicates that the fuzzy entropy increases firstly and then decreases as the mode dimension p changes from 1 to 10, and it reaches the maximum value when the mode dimension p is 2. Therefore, the value of mode dimension p in equation (12) is chosen as 2.

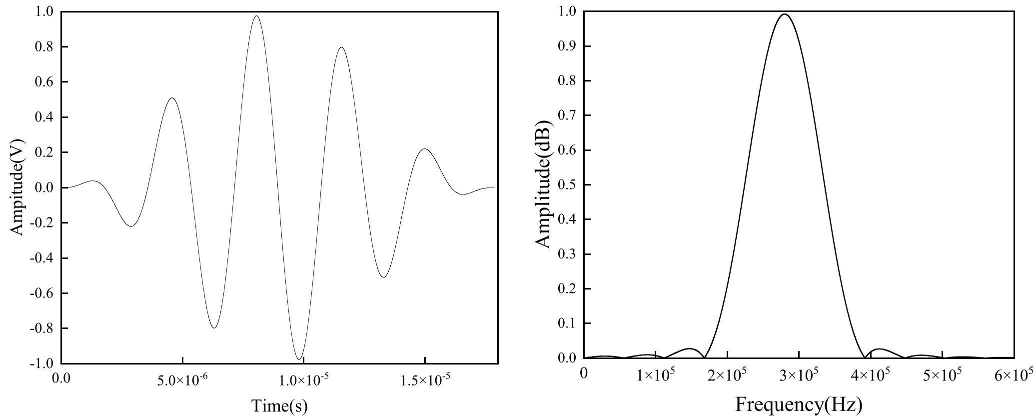

(a) Time domain (b) Frequency domain

Figure 4. The 280 kHz five-cycle sinusoidal pulse tuned by a Hanning window.

Table 2. Locations of the simulated damages.

Location of the damage	Coordinate (mm, mm)
A	(105, 45)
B	(46, 0)
C	(95, −97)

Table 3. Different types of the simulated damages.

No.	Damage type		Location of the magnets	Number of the magnets	Total number of the magnets
1	Without damage	M0	/	/	0
2	Single damage	A1	A	1	1
3		A2	A	2	2
4		A3	A	3	3
5		A4	A	4	4
6		B1	B	1	1
7		B2	B	2	2
8		B3	B	3	3
9		B4	B	4	4
10		C1	C	1	1
11		C2	C	2	2
12		C3	C	3	3
13		C4	C	4	4
14	Multi-damage	M1	A	1	2
			B	1	
15		M2	A	1	3
			B	1	
			C	1	
16		M3	A	2	3
			B	1	

4.2. Influence of SSA on the normalized fuzzy entropy

Figure 7 plots the curves of the normalized fuzzy entropy with and without SSA. Figure 7 clearly shows that the normalized fuzzy entropy with SSA has a much larger variation than that without SSA as the damage changes, which indicates that SSA is helpful to extract the nonlinear features of different damages during the detection.

4.3. Influence of the propagating path of ultrasonic waves on the normalized fuzzy entropy

Figure 8 shows the time-domain signals of different damages, and PZT 1 and PZT 2 are the actuator and sensor, respectively. Figure 8 shows that the four signals of different damages are nearly the same, which indicates that the simulated damages cannot be identified directly by the time-domain signals.

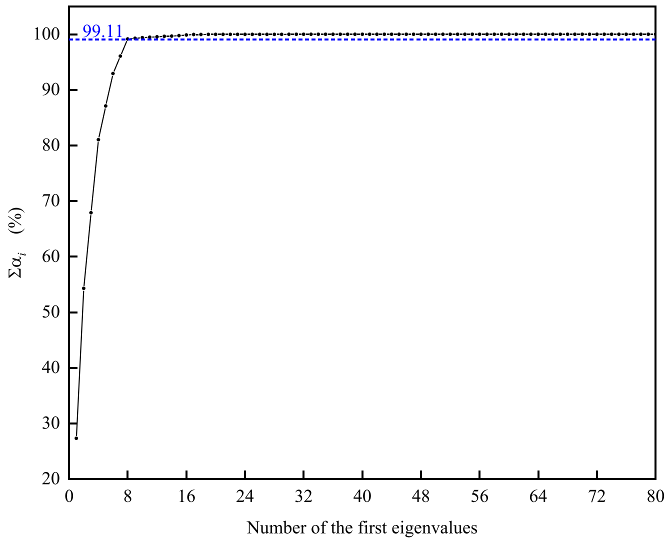

Figure 5. The summation of the ratio α_i of the first i eigenvalue.

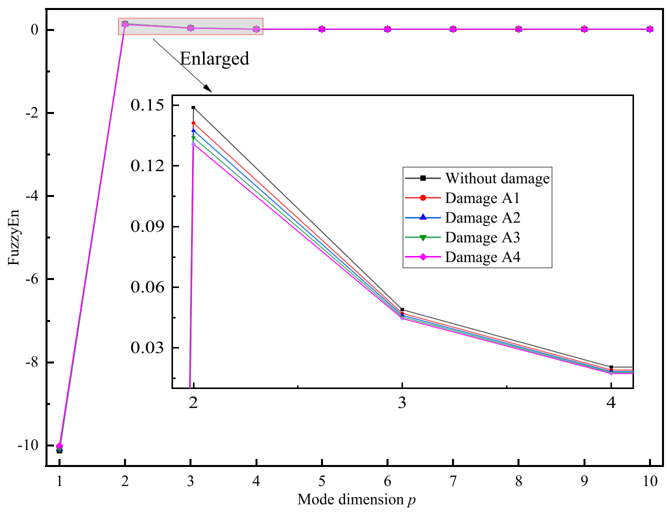

Figure 6. Influence of the mode dimension p on the fuzzy entropy of different damages.

Figure 9 plots curves of the normalized fuzzy entropy of different damages by using different actuator–sensor pairs. Figure 9 shows that the normalized fuzzy entropy of damage M0, i.e. without added mass on the plate, is larger than those of others (damages A1–A3). That is because the presence of the added mass makes the movement of the points near the mass more difficult, and some modes of Lamb waves, which have low relevance in the vibration, is disturbed. Eventually, more energy goes to the domain modes, and the complexity and nonlinearity of the waves are weakened by the disturbed ones [52]. Therefore, the entropy, which reflects the complexity and nonlinearity of the system, decreases. Figure 9 also shows that the changing trend of the normalized fuzzy entropy is nearly the same when both the actuator and damage type are the same, which indicates that the propagating path of the ultrasonic waves has a very limited influence on the normalized fuzzy entropy.

4.4. Detection of severity of damages on the same location

Figure 10 plots the normalized fuzzy entropy of different damages (A1–A4, B1–B4 and C1–C4) on the locations A, B and C, respectively. Figure 10 shows that when the location of the damage remains the same, the normalized fuzzy entropy decreases linearly as the severity of the damage, i.e. the number of the magnets, increases, which demonstrates that the proposed normalized fuzzy entropy can be used to detect the severity of the damage on the same location. The explanation of the changing trend may be that when the number of the magnets increases, the total mass of the added magnets increases, and the disturbance to the movement and some vibration modes of Lamb waves becomes greater. Therefore, the nonlinearity of the waves gets weaker, and the fuzzy entropy decreases as the number of the magnets increases.

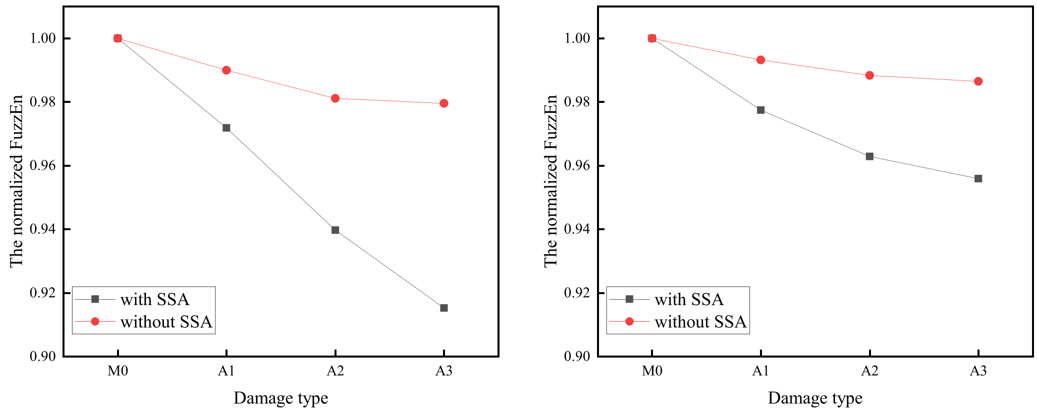

(a) PZT 1 - actuator, PZT 4 - sensor (b) PZT 1 - actuator, PZT 8 - sensor

Figure 7. Comparison of the normalized fuzzy entropy with and without SSA.

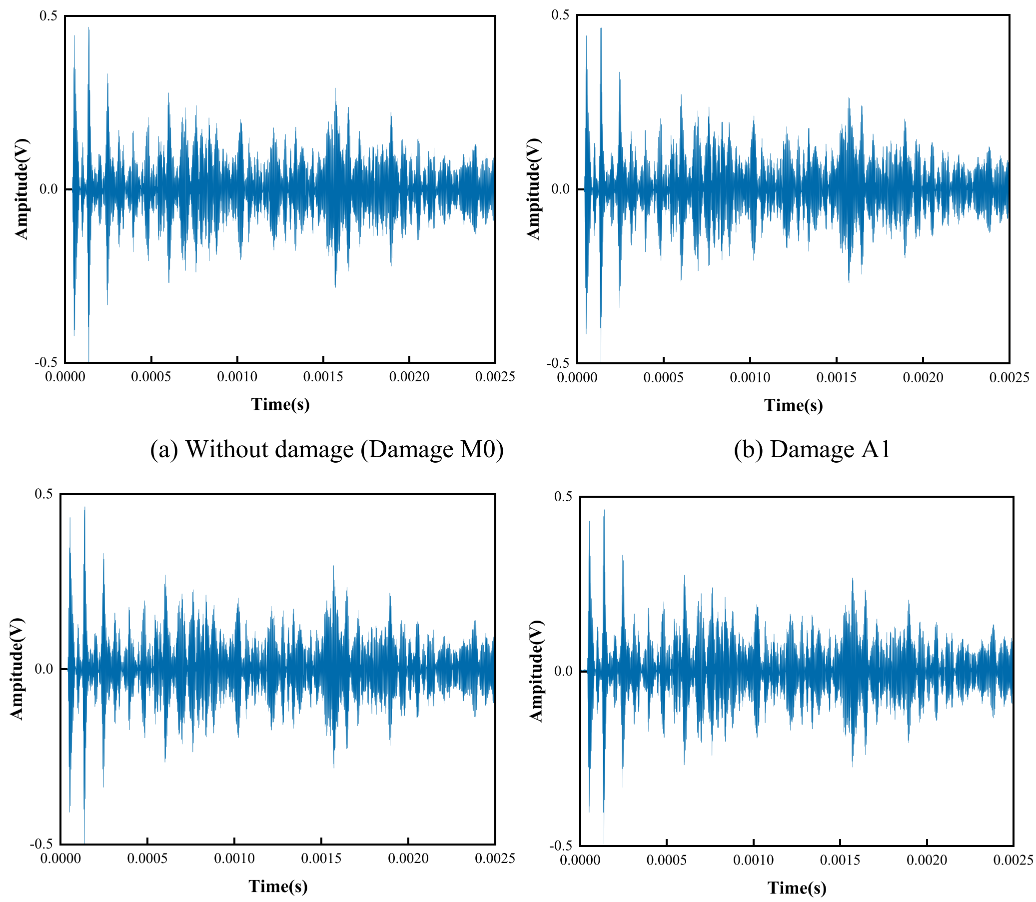

(a) Without damage (Damage M0) (b) Damage A1

(c) Damage A2 (d) Damage A3

Figure 8. Time-domain signals with different damages (PZT 1—actuator, PZT 2—sensor).

4.5. Detection of severity of multi-damages on different locations

Figure 11 plots the normalized fuzzy entropy of both the single and multi-damages (A1–A3 and M1–M3).

Figure 11 clearly shows that the normalized fuzzy entropy of the multi-damages (M0–M3) changes as the type of the damage changes, which indicates that the proposed entropy also can be employed to identify the multi-damages.

By comparing the normalized fuzzy entropy of both the single and the multi-damages (A1–A3 and M1–M3) in figure 11, it also demonstrates that the normalized fuzzy entropy is relevant with the total number and location of the added magnets. The entropy decreases as the total number of

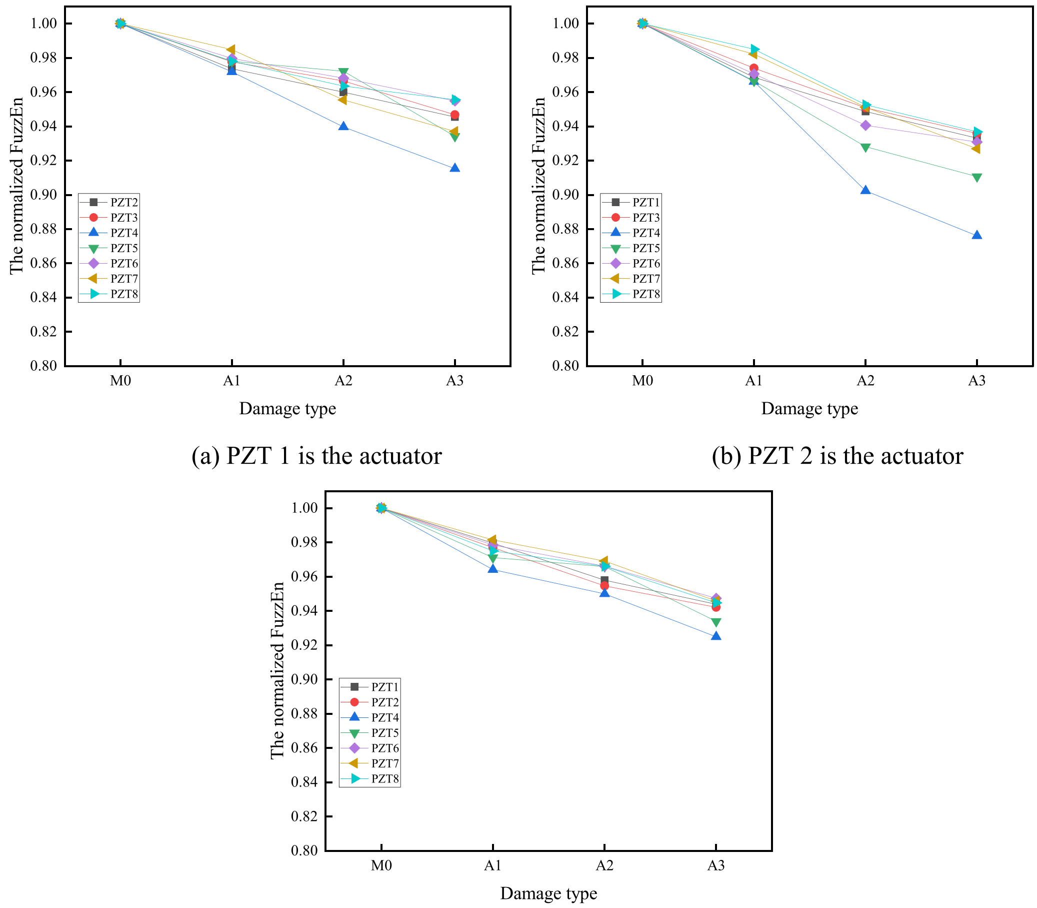

(a) PZT 1 is the actuator

(b) PZT 2 is the actuator

(c) PZT-3 is the actuator

Figure 9. The normalized fuzzy entropy of different damages by using different actuator–sensor pairs.

the added magnets increases. Moreover, when the total number of the added magnets is the same, the normalized fuzzy entropy of the multi-damage is larger than that of the single damage.

4.6. Comparison of the simulation results

A finite element simulation is also conducted to compare the performance of the proposed method. The dimensions of the plate, PZTs and the added mass are the same as shown in figure 3 and their locations are given in section 3. The added mass is set as a rigid body and the weight of each mass is 4.4 g. In the model, the PZTs and added mass are glued to the aluminium plate. The mesh size is set to be 0.5–1.5 mm, and the 3D finite element model is shown in figure 12. The material parameters are listed in table 4. In the simulation, the excitation pulse is the same as the experiments and its amplitude is 1 V, and the time step is set to be 0.5 μs.

Figure 13 displays the time-domain signals obtained by simulations, and PZT 1 and PZT 2 are the actuator and sensor, respectively. Figure 14 plots the normalized fuzzy entropy of different damages (A1–A3) on the location A by finite element analysis. Figure 13 shows that the normalized fuzzy entropy of the simulation also decreases as the severity of the damage, i.e. the number of the magnets, increases. Compared with figure 9(a), figure 13 also demonstrates that the changing trend of the simulation results is consistent with the experimental one.

4.7. Discussions

In this section, the proposed SSA and fuzzy entropy-based method is used to detect the added magnets on one or more locations of the aluminium plate, and the experimental results are analysed. Since the movement and some vibration modes of Lamb waves near to the magnets are disturbed by the added magnets, the complexity and nonlinearity of the received waves are weakened, and therefore the normalized fuzzy entropy is smaller than that when there are no magnets on the plate. Moreover, the more the number of the magnets is, the greater the influence of the magnets is and the smaller the entropy is. When the same total number of magnets are placed on two or more different locations, the disturbing effect on the waves is stronger than that when they are only placed on one location. Eventually, the normalized fuzzy entropy of multi-damage is less than that of a single damage for the same number of magnets. Moreover, the experimental results are consistent with the simulation results. The experimental results

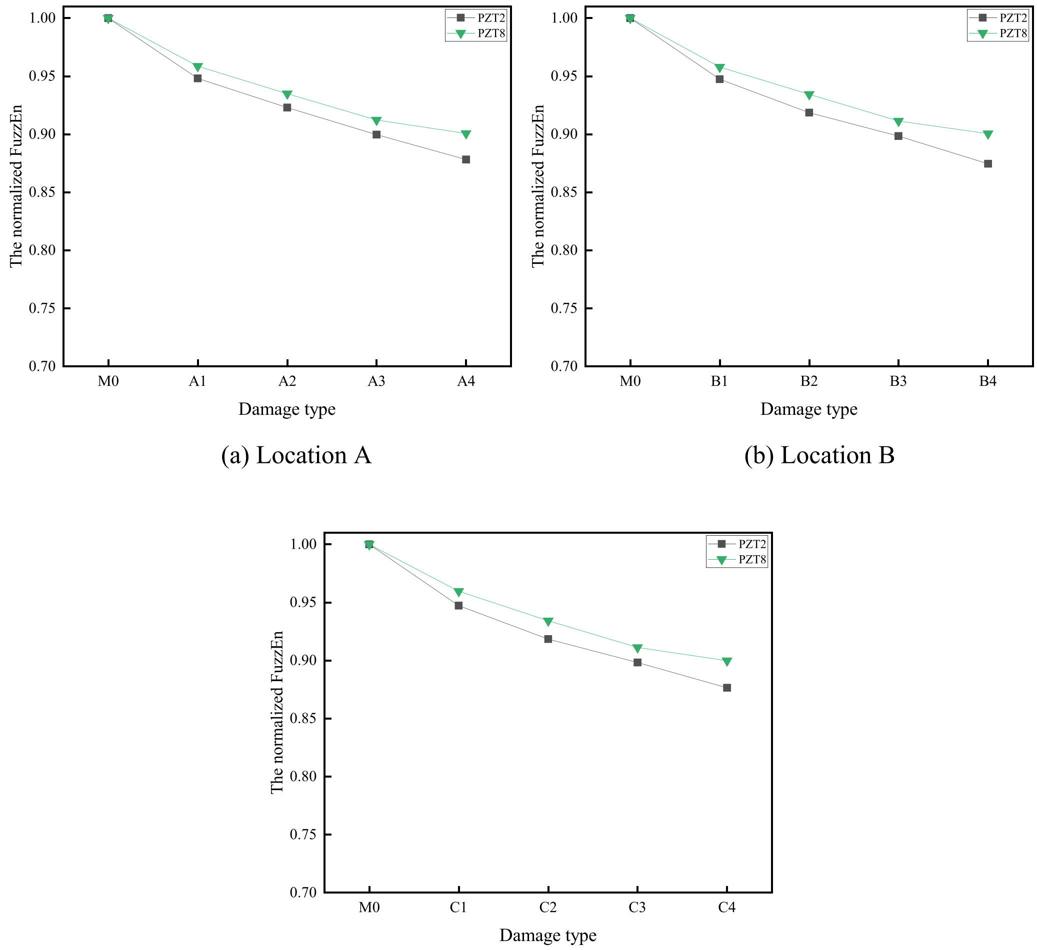

(a) Location A

(b) Location B

(c) Location C

Figure 10. The normalized fuzzy entropy with a single damage on locations A, B and C (PZT-1 is the actuator).

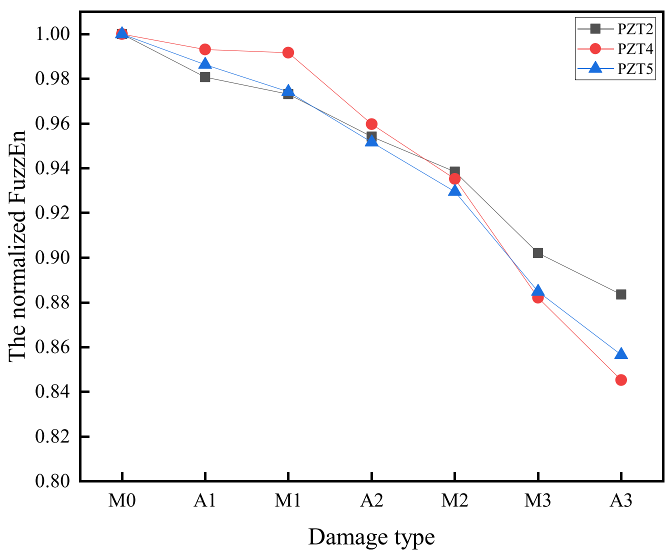

Figure 11. The normalized entropy of single and multi-damages on different locations (PZT-1 is the actuator).

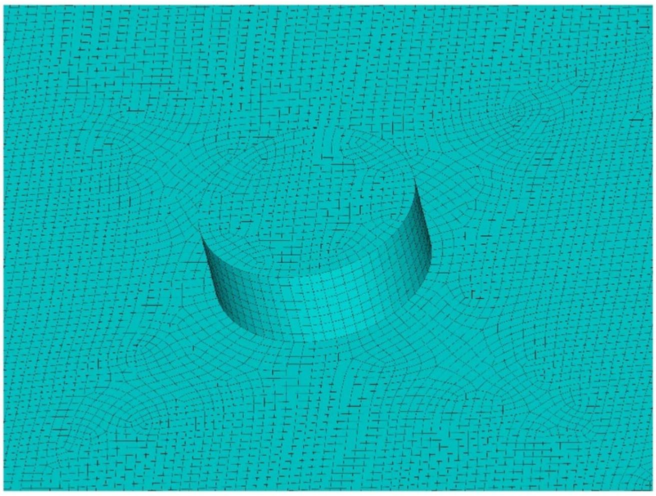

Figure 12. The 3D finite element model.

Table 4. Material parameters of the aluminium plate and PZTs.

Material	Aluminium 6061	PZT-5
Density ρ (kg m^{-3})	2700	7800
Young's modulus E (GPa)	68.9	53
Poisson ratio ν	0.33	0.34
Piezoelectric strain coefficients $d_{31}/d_{33}/d_{15}$ (10^{-12} m V^{-1})	/	$-150/400/640$
Relative permittivity ε_r	/	1600

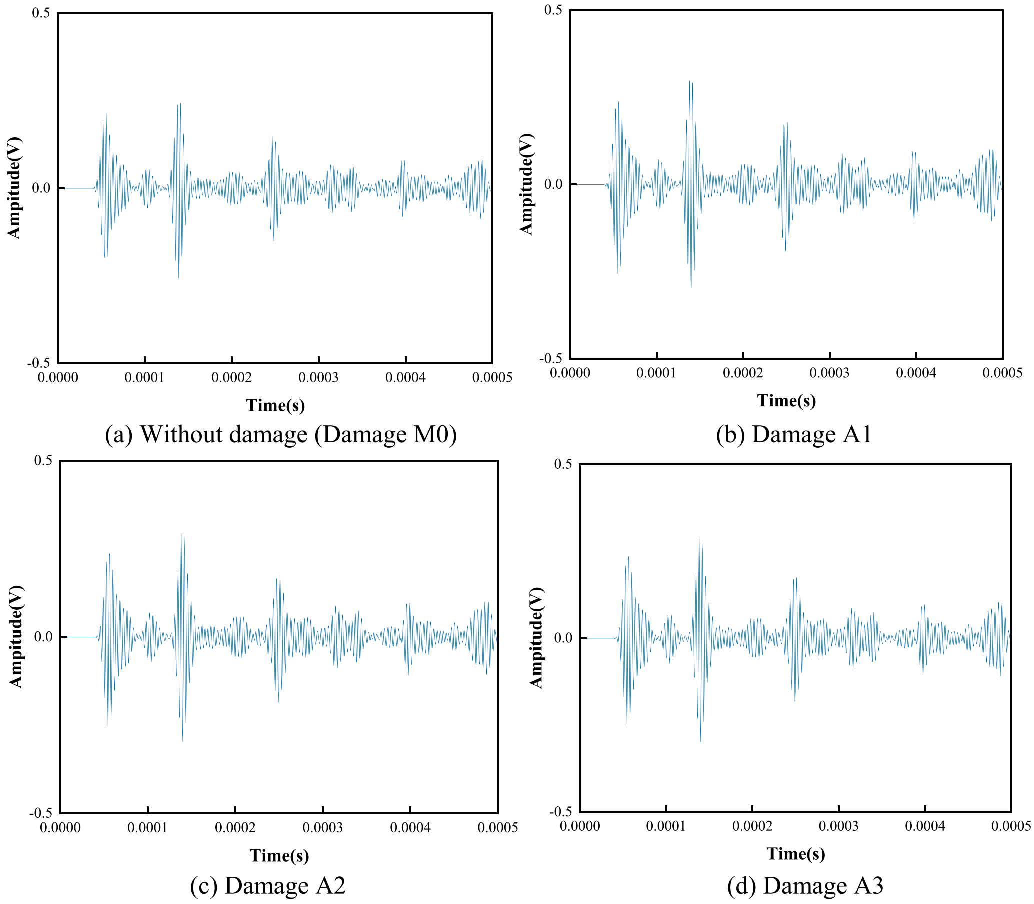

Figure 13. Time-domain signals with different damages (PZT 1—actuator, PZT 2—sensor).

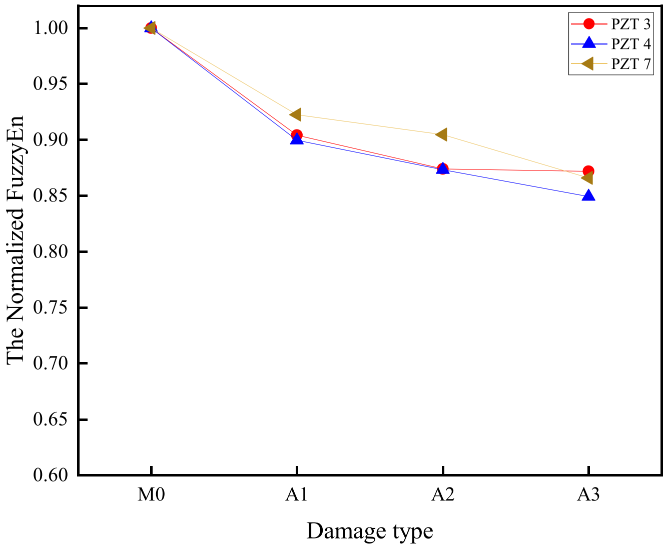

Figure 14. The normalized entropy of different damages in the simulations (PZT-1 is the actuator).

validate that the proposed method can be used to detect both the single and multiple added magnets on a thin plate.

5. Conclusions

In this research, a new method based on SSA and fuzzy entropy is developed for damage detection of thin wall-like structures, and the normalized fuzzy entropy is employed as an indicator to identify the severity of the damage. During the detection, the collected signals are firstly decomposed and reconstructed by SSA to extract the feature of the damage, and then the reconstructed signals with the feature of the damage are processed to obtain the normalized fuzzy entropy. An experimental setup is fabricated to validate the proposed method. Since the movement and some vibration modes of Lamb waves near the location of the added mass is disturbed by the existence of the added mass, the complexity and nonlinearity of the waves are weakened, and therefore the experimental results show that the normalized fuzzy entropy of damage M0, i.e. without added mass on the plate, is larger than those of others (damages A1–A3). The experimental results of a single damage with different number of magnets (damages A1–A4, B1–B4 and C1–C4) indicate that the normalized fuzzy entropy decreases linearly as the number of the added magnets increases, which demonstrates that the proposed method can be used to detect the severity of the damage. The explanation of this changing trend may be that when the number of the magnets increases, the total mass of the added magnets increases, and the disturbance to the movement and some vibration modes of Lamb waves becomes greater. Moreover, the experimental results of multi-damages on different locations (damages M1–M3) indicate that the normalized fuzzy entropy is relevant with both the total number and locations of the added magnets. The normalized fuzzy entropy decreases linearly as the total number of the magnets increases, and the entropy of a single damage is smaller than that of the multi-damage with the same total number of magnets, which demonstrates that the proposed method also can be used for multi-damage detection on a thin plate.

This study provides us a new approach to identifying the single and multiple damages on thin wall-like structures. As an outlook, the discrimination ability of this method can be improved by introducing some machine learning classifier algorithms. Future work involves damage detection of more different types of damage, such as fatigue crack, delamination and corrosion, and it also involves damage location identification based on SSA and fuzzy entropy. Also, the influence of the damage on the complexity of waves needs more in-depth investigations.

Data availability statement

The data that support the findings of this study are available upon reasonable request from the authors.

Acknowledgment

The authors are grateful for the financial support from National Natural Science Foundation of China (Grant No. 51808417).

ORCID iDs

Guangtao Lu https://orcid.org/0000-0002-6505-6916
Tao Wang https://orcid.org/0000-0003-4591-0123

References

[1] Zhang C, Wang R and Song G 2020 Post-fire mechanical properties of Q460 and Q690 high strength steels after fire-fighting foam cooling *Thin Wall. Struct.* **156** 106983
[2] Feng R, Zhang R, Li S, Kong G and Zhu X 2012 Study on forming mechanism of lamination defect of AH36 shipbuilding plate steel *Adv. Mater. Res.* **562–564** 106–10
[3] Zhao G, Huang Q, Zhou C, Zhang Z, Ma L and Wang X 2016 Experiment and simulation analysis of roll-bonded Q235 steel plate *Rev. Metal.* **52** e069
[4] Xu W, Cao M, Su Z, Xu H, Radzieński M and Ostachowicz W 2021 Imaging delamination in composite laminates using perturbation to steady-state wavefields *Smart Mater. Struct.* **30** 075023
[5] Zhao C, Zhu H and Wang X 2019 Steel plate surface defect recognition method based on depth information *2019 IEEE 8th Data Driven Control and Learning Systems Conf. (DDCLS)*
[6] Jiménez-Peña C, Goulas C, Rossi B and Debruyne D 2019 Influence of hole-making procedures on fatigue behaviour of high strength steel plates *J. Constr. Steel Res.* **158** 1–14
[7] Lu G, Li Y and Song G 2016 A delay-and-Boolean-ADD imaging algorithm for damage detection with a small number of piezoceramic transducers *Smart Mater. Struct.* **25** 095030
[8] Xie J, Xu C, Chen G and Huang W 2018 Improving visibility of rear surface cracks during inductive thermography of metal plates using Autoencoder *Infrared Phys. Technol.* **91** 233–42

[9] Feng F, Zhang C, Min Q, Zhu J, Wang W and Chao X 2017 Heating characterization of the thickness-through fatigue crack in metal plate using sonic IR imaging *NDT&E Int.* **87** 38–43
[10] Mentyukov K Y, Bortsov A, Shabalov I and Mansyrev E 2016 Study of the properties of the base metal of large-diameter pipes under alternating loading *Metallurgist* **60** 397–404
[11] Kim S H, Kim J G and Kim W C 2017 Effect of crevice former on the corrosion behavior of 316L stainless steel in chloride-containing synthetic tap water *CORROSION 2017*
[12] Peng J, Xiao L, Zhang J, Cai C and Wang L 2019 Flexural behavior of corroded HPS beams *Eng. Struct.* **195** 274–87
[13] Lugauskas A, Prosycevas I, Ramanauskas R, Griguceviciene A, Selskiene A and Pakstas V 2009 The influence of micromycetes on the corrosion behaviour of metals (steel, Al) under conditions of the environment polluted with organic substances *Mater. Sci.* **15** 224–35
[14] Zeng X, Liu X and Sun H 2021 Prognosis of fatigue cracks in an aircraft wing using an adaptive tunable network and guided wave based structural health monitoring *Smart. Mater. Struct.* **30** 105025
[15] Zhang G, Gao W, Song G and Song Y 2016 An imaging algorithm for damage detection with dispersion compensation using piezoceramic induced lamb waves *Smart Mater. Struct.* **26** 025017
[16] Yan S, Zhang B, Song G and Lin J 2018 PZT-based ultrasonic guided wave frequency dispersion characteristics of tubular structures for different interfacial boundaries *Sensors* **18** 4111
[17] Wang F, Ho S C M and Song G 2019 Monitoring of early looseness of multi-bolt connection: a new entropy-based active sensing method without saturation *Smart Mater. Struct.* **28** 10LT01
[18] Zhang Y, Tournat V, Abraham O, Durand O, Letourneur S, le Duff A and Lascoup B 2013 Nonlinear mixing of ultrasonic coda waves with lower frequency-swept pump waves for a global detection of defects in multiple scattering media *J. Appl. Phys.* **113** 064905
[19] Wimarshana B, Wu N and Wu C 2017 Crack identification with parametric optimization of entropy & wavelet transformation *Struct. Monit. Maint.* **4** 33–52
[20] Lee S G, Yun G J and Shang S 2014 Reference-free damage detection for truss bridge structures by continuous relative wavelet entropy method *Struct. Health Monit.* **13** 307–20
[21] HosseinAbadi H Z, Amirfattahi R, Nazari B, Mirdamadi H R and Atashipour S A 2014 GUW-based structural damage detection using WPT statistical features and multiclass SVM *Appl. Acoust.* **86** 59–70
[22] Bhowmik B, Tripura T, Hazra B and Pakrashi V 2020 Real time structural modal identification using recursive canonical correlation analysis and application towards online structural damage detection *J. Sound Vib.* **468** 115101
[23] Torkamani S, Roy S, Barkey M E, Sazonov E, Burkett S and Kotru S 2014 A novel damage index for damage identification using guided waves with application in laminated composites *Smart Mater. Struct.* **23** 095015
[24] Chen H, Zhang G, Fan D, Fang L and Huang L 2020 Nonlinear Lamb wave analysis for microdefect identification in mechanical structural health assessment *Measurement* **164** 108026
[25] Zeng L, Huang L, Cao X and Gao F 2019 Determination of Lamb wave phase velocity dispersion using time–frequency analysis *Smart Mater. Struct.* **28** 115029
[26] Wang Z, Qiao P and Shi B 2018 Effective time-frequency characterization of Lamb wave dispersion in plate-like structures with non-reflecting boundaries *Smart Struct. Syst.* **21** 195–205
[27] Xu B, Yuan S, Wang M and Qiu L 2015 Determining impact induced damage by lamb wave mode extracted by EMD method *Measurement* **65** 120–8
[28] Barbosh M, Sadhu A and Sankar G 2021 Time–frequency decomposition-assisted improved localization of proximity of damage using acoustic sensors *Smart Mater. Struct.* **30** 025021
[29] Zhong Y, Xiang J, Chen X, Jiang Y and Pang J 2018 Multiple signal classification-based impact localization in composite structures using optimized ensemble empirical mode decomposition *Appl. Sci.* **8** 1447
[30] Li R, Luo J and Hu B 2020 Lamb wave-based damage localization feature enhancement and extraction method for stator insulation of large generators using VMD and wavelet transform *Sensors* **20** 4205
[31] Yelve N P, Mitra M and Mujumdar P M 2014 Spectral damage index for estimation of breathing crack depth in an aluminum plate using nonlinear Lamb wave *Struct. Control Health. Monit.* **21** 833–46
[32] Sun F, Wang N, He J, Guan X and Yang J 2017 Lamb wave damage quantification using GA-based LS-SVM *Materials* **10** 648
[33] Zheng K, Li Z, Ma Z, Chen J, Zhou J and Su X 2019 Damage detection method based on Lamb waves for stiffened composite panels *Compos. Struct.* **225** 111137
[34] Cho H, Hasanian M, Shan S and Lissenden C J 2019 Nonlinear guided wave technique for localized damage detection in plates with surface-bonded sensors to receive Lamb waves generated by shear-horizontal wave mixing *NDT&E Int.* **102** 35–46
[35] Nasser J, Groo L and Sodano H A 2021 Artificial neural networks and phenomenological degradation models for fatigue damage tracking and life prediction in laser induced graphene interlayered fiberglass composites *Smart Mater. Struct.* **30** 085010
[36] Wang F 2021 Identification of multi-bolt head corrosion using linear and nonlinear shapelet-based acousto-ultrasonic methods *Smart Mater. Struct.* **30** 085031
[37] Krishnasamy L, Arumulla R M R and Naga G 2018 An improved damage diagnostic technique based on singular spectrum analysis and time series models *Struct. Infrastruct.* E **14** 1412–31
[38] Liu L and Yan Y 2015 Singular spectrum analysis and its application in Lamb wave-based damage detection *J. Vibroeng.* **17** 3561–71
[39] de Oliveira M A, Vieira Filho J, Lopes J V and Inman D J 2017 A new approach for structural damage detection exploring the singular spectrum analysis *J. Intell. Mater. Syst. Struct.* **28** 1160–74
[40] Moreno-Gomez A, Amezquita-Sanchez J, Valtierra-Rodriguez M, Perez-Ramirez C, Dominguez-Gonzalez A and Chavez-Alegria O 2018 EMD-Shannon entropy-based methodology to detect incipient damages in a truss structure *Appl. Sci.* **8** 2068
[41] Ceravolo R, Civera M, Lenticchia E, Miraglia G and Surace C 2020 Damage detection and localisation in buried pipelines using entropy in information theory *1st Int. Electronic Conf. on Applied Sciences*
[42] Ceravolo R, Civera M, Lenticchia E, Miraglia G and Surace C 2021 Detection and localization of multiple damages through entropy in information theory *Appl. Sci.* **11** 5773
[43] Xie Z K, Liu G H and Zhang Z H 2012 Damage detection of concrete structure based on approximate entropy *Appl. Mech. Mater.* **226–228** 920–5
[44] Ni Q, Feng K, Wang K, Yang B and Wang Y 2017 A case study of sample entropy analysis to the fault detection of bearing in wind turbine *Case Stud. Eng. Fail. Anal.* **9** 99–111
[45] Wang F, Zheng C and Song G 2020 Monitoring of multi-bolt connection looseness using entropy-based active sensing

and genetic algorithm-based least square support vector machine *Mech. Syst. Signal Process.* **136** 106507
[46] Rojas E, Baltazar A and Loh K J 2015 Damage detection using the signal entropy of an ultrasonic sensor network *Smart Mater. Struct.* **24** 075008
[47] Burud N and Kishen J M C 2020 Damage detection using wavelet entropy of acoustic emission waveforms in concrete under flexure *Struct. Health Monit.* 1475921720957096
[48] Lin T K and Laínez A G 2018 Entropy-based structural health monitoring system for damage detection in multi-bay three-dimensional structures *Entropy* **20** 49
[49] Lin T K and Liang J C 2015 Application of multi-scale (cross-) sample entropy for structural health monitoring *Smart Mater. Struct.* **24** 085003
[50] Lin T K and Huang T H 2020 Damage quantification of 3D-printed structure based on composite multiscale cross-sample entropy *Smart Mater. Struct.* **30** 015015
[51] Chang Y, Yang D and Guo Y 2018 Laser ultrasonic damage detection in coating-substrate structure via Pearson correlation coefficient *Surf. Coat. Technol.* **353** 339–45
[52] Castro E, Moreno-García P and Gallego A 2014 Damage detection in CFRP plates using spectral entropy *Shock Vib.* **2014** 693593
[53] Hassani H 2007 Singular spectrum analysis: methodology and comparison *J. Data Sci.* **5** 239–57
[54] Vautard R and Ghil M 1989 Singular spectrum analysis in nonlinear dynamics, with applications to paleoclimatic time series *Physica* D **35** 395–424
[55] Schoellhamer D H 2001 Singular spectrum analysis for time series with missing data *Geophys. Res. Lett.* **28** 3187–90
[56] Golyandina N, Nekrutkin V and Zhigljavsky A A 2001 *Analysis of Time Series Structure: SSA and Related Techniques* (London: Chapman and Hall/CRC)
[57] Chen W, Wang Z, Xie H and Yu W 2007 Characterization of surface EMG signal based on fuzzy entropy *IEEE Trans. Neural Syst. Rehabil. Eng.* **15** 266–72
[58] Zheng J, Pan H and Cheng J 2017 Rolling bearing fault detection and diagnosis based on composite multiscale fuzzy entropy and ensemble support vector machines *Mech. Syst. Signal Process.* **85** 746–59
[59] Kong Q, Robert R H, Silva P and Mo Y 2016 Cyclic crack monitoring of a reinforced concrete column under simulated pseudo-dynamic loading using piezoceramic-based smart aggregates *Appl. Sci.* **6** 341
[60] Ji Q, Ding Z, Wang N, Pan M and Song G 2018 A novel waveform optimization scheme for piezoelectric sensors wire-free charging in the tightly insulated environment *IEEE Internet Things* **5** 1936–46
[61] Kong Q, Hou S, Ji Q, Mo Y and Song G 2013 Very early age concrete hydration characterization monitoring using piezoceramic based smart aggregates *Smart Mater. Struct.* **22** 085025
[62] Huo L, Cheng H, Kong Q and Chen X 2019 Bond-slip monitoring of concrete structures using smart sensors—a review *Sensors* **19** 1231
[63] Huo L, Li C, Jiang T and Li H 2018 Feasibility study of steel bar corrosion monitoring using a piezoceramic transducer enabled time reversal method *Appl. Sci.* **8** 2304
[64] Lamb H 1917 On waves in an elastic plate *Proc. R. Soc.* A **93** 114–28
[65] Worlton D 1961 Experimental confirmation of Lamb waves at megacycle frequencies *J. Appl. Phys.* **32** 967–71
[66] Zhang X and Wang J 2018 A novel decomposition-ensemble model for forecasting short-term load-time series with multiple seasonal patterns *Appl. Soft Comput.* **65** 478–94